MR Imaging of Rectal Cancer using Endorectal Surface Coil: Histopathological Correlation

Yutaka Imai

Department of Radiology, Keio University School of Medicine

直腸内コイルを用いた直腸癌のMRI －病理組織像との対比－

今井　裕

近年の直腸癌に対する外科的治療法の進歩は，正確な腫瘍の解剖学的な位置と病期診断を必要としている．われわれは受信専用のMRI用直腸内コイルを開発し，これを用いて直腸癌55病変に対して腫瘍の深達度およびリンパ節転移の有無について診断した．術前のMRI所見は，切除後に病理組織像と対比し検討した．なお，早期癌と思われた最近の11例では，内視鏡にて粘膜下層に生理的食塩水を局注してから撮影した．

正常の腸管壁はFSEのT2強調像にて表層の粘液および周囲脂肪織も含めて5～6層に分かれて描出され，粘膜層は低信号，粘膜下層は高信号，固有筋層は低信号を示した．腫瘍の深達度診断については，T2強調像ではm癌は粘膜層の肥厚，sm癌は高信号域内の低信号の腫瘤や腫瘍と粘膜下層との境界の不整さとして描出された．腫瘍が固有筋層へ浸潤すると，粘膜下層は完全に断裂し，筋層の肥厚，断裂，あるいは筋層内の高信号を示す腫瘤として認められた．さらに腫瘍が周囲脂肪織に浸潤するとT1強調像にて腫瘍外側辺縁は不整となり，T2強調像では低信号を示す外縦筋層の断裂として診断された．

MRI所見は55例中45例(81.8％)において病理組織像と良く一致した．また，生理的食塩水の局注は菲薄な粘膜下層を肥厚させるため，治療法の選択において重要なm癌および粘膜下浸潤が少量のsm_1癌と粘膜下層へ多量に浸潤する$sm_{2\sim3}$癌との鑑別に有用であった．直腸内コイルのMR画像を含めたリンパ節転移の診断能は，sensitivityは78.9％，specificityは74.1％であり，径5mm前後のリンパ節の形状も評価することができた．

直腸内コイルを用いたMRIは，正常の腸管壁の層構造を描出し，腫瘍の壁内浸潤や少量の壁外浸潤の診断，さらに小さなリンパ節転移の拾い上げが可能となり，直腸癌の治療法の選択に重要な情報を提供できると考えられた．

Research Code No. : 513.9

Key words : *Magnetic resonance imaging (MRI), Endorectal coils, Rectal cancer, Submucosal saline injection, Tumor staging*

Received Jan. 5, 1999; revision accepted May 20, 1999

慶應義塾大学医学部放射線科学教室

Introduction

Recent advances in surgical and endoscopic treatments for rectal cancer demand more accurate preoperative assessment of both tumor localization and staging[1)-4)]. Local resection or endoscopic polypectomy can be applied if there is reasonable certainty that no lymph node metastasis exists or that a tumor does not massively infiltrate the submucosa. The indications of laparoscopic colectomy are tumor infiltration limited to the submucosa and no evidence of lymph node metastasis. The differentiation between tumors confined to the intestinal wall and those with extramural infiltration also makes a difference in surgical planning, especially in the autonomic nerve-preserving operation[5)]. The purpose of this study was to assess the potential of endorectal MR imaging in defining the extent of colorectal cancers and to discuss the practical aspects of this procedure.

Patients and Methods

Fifty-five patients with rectal cancer were examined with MR imaging using endorectal surface coils. All the patients underwent barium enema and colonoscopy before MR imaging. Lesion sizes ranged from 1.0 cm to 7.0 cm (average 3.3 cm) in maximum diameter. The distances between the lesions and the anal verge ranged from 3.0 cm to 14.0 cm (average 6.7 cm). The distribution of lesions was as follows: lower rectum (Rb) 34 cases, middle part (Ra) 19 cases, and upper part (Rs) 2 cases.

MR imaging was performed with a 1.5 Tesla superconducting MR unit (Signa; GE Medical Systems, Milwaukee, WI) using tailored endorectal surface coils and fast spin echo (FSE) capabilities. Several kinds of endorectal coils were fashioned in our own laboratory to accommodate various anatomic requirements. The basic design of these coils was similar to a double-balloon prostate probe (MEDRAD, Pittsburgh). The inner balloon, ellipsoidal and flat in shape, works to distend the flexible coil, while the outer balloon, made of soft rubber, provides complete waterproofing. The coil shaft is made of a flexible silicone tube instead of common stiff materials (Fig. 1). In six cases, the endorectal coil was used with external

Fig. 1 An endorectal surface coil is sandwiched between the outer and inner balloons. An appropriate coil is chosen from a variety of sizes, 6 × 3 cm to 12 × 6 cm, to accommodate different anatomical requirements. The shape of the balloon is ellipsoidal rather than circular in cross-section so as to keep the coil closer to the lesion.

coils as part of the endorectal-external multi-coil array.

After the body-coil or phased-array pelvic coil images were obtained in search of distant lymph node metastasis, endorectal MR imaging was performed. Information provided by the preceding barium study or endoscopic examination was used to place the flexible endorectal coil in direct contact with the lesion.

In 28 of 55 cases, the endorectal coil was inserted up to the lesion without difficulty. In 20 cases, 500 ml of air was infused to inflate the bowel lumen before insertion of the coil. In seven cases, an endoscope was used to guide the endorectal coil, since tumors were located at the recto-sigmoid junction where the rectum would course with a steep angulation. In 11 cases in which the lesion size was up to 2.0 cm in diameter with any surface configuration or up to 2.5 cm in diameter without central ulceration, the submucosal injection of saline was performed by endoscope prior to the insertion of the endorectal coil. In seven cases, the endorectal coil was guided to the lesion with the assistance of an endoscope. In two patients with severe rectal stenosis due to a bulky, annular tumor, the endorectal coil could not be placed properly, and these two cases were removed from this study.

Antispasmodic agents (n-butylscopolamin or glucagon) were intramuscularly used prior to imaging, to reduce motion artifacts. Flatus enema was applied one hour prior to the examination. The diagnosis of tumor staging and lymph node metastasis was prospectively made on the day of MR examination, before tumor resection.

After sagittal images with a 30-cm field of view had been obtained for localization, spin echo T1-weighted images, 400/12 or 15/2 (TR/TE/excitations), and FSE T2-weighted images, 3700/104/2 or 4/12 (TR/TE/excitations/echo trains), were acquired with an 8- to 12-cm field of view, 4-mm slice thickness, and 256 × 192 matrix. In all cases, sagittal, coronal, or oblique sections perpendicular to the rectal wall were obtained in addition to the routine axial images. Gd-DTPA (0.1 mmol/kg) was intravenously administered by bolus injection in 55 cases.

Surgical resection was done within 14 days after MR imaging. All specimens were directly fixed in 10% formalin, and 40 of them were imaged with a 3-inch-diameter surface coil *ex vivo* before sectioning for histopathological correlation. In every case, a thin string was attached to the specimen along the landmark-beam of the scanner, so that the identical sectional planes were produced with microtome cutting for proper MRI-histopathological correlation. These sections were stained with hematoxylin-eosin. MR images, both *in vivo* and *ex vivo*, were correlated with the histopathological findings.

Rectal carcinomas with submucosal invasion (T1 stage) were histopathologically divided into three subtypes, sm_1, sm_2 and sm_3, in this study. The definition of sm1 was set as up to 500 μm, sm_2 up to 2000 μm, and sm_3 over 2001 μm in distance from the muscularis mucosa to the deepest tumor invasion.

MRI Criteria for Tumor Staging

Carcinomas limited to the mucosa were classified as M-carcinoma, and carcinomas involving the submucosa as SM-carcinoma. Carcinomas spreading into the muscularis propria were MP-carcinoma, and carcinomas penetrating through the muscularis propria were S (A)-carcinoma. M-carcinoma is categorized as Tis-stage in the TNM staging system[6], and similarly, SM-carcinoma as stage T1, MP-carcinoma as T2, and S (A)-carcinoma as T3. SM carcinomas (T1 stage) were subdivided into minute submucosal invasion (SM_1) and massive submucosal invasion ($SM_{2\sim3}$) in MRI diagnosis.

We applied the same assessment to the extent of tumor invasion in this *in vivo* study with endorectal surface coils as that used in the *ex vivo* study[7] (Table 1). MRI diagnoses of the depth of carcinomatous invasion were divided into four groups, as follows: M- and SM_1-carcinoma: the discrete thickening of the inner hypointense layer and the interface between the tumor and the next hyperintense layer is smooth on the T2-weighted image; $SM_{2\sim3}$-carcinoma: a low signal intensity mass in the middle hyperintense layer; MP carcinoma: discontinuity of the middle hyperintense layer, and thickening of the

Table 1 Assessment of depth of carcinomatous invasion by endorectal MRI

Stage	T1-weighted image	T2-weighted image
M, SM_1		Thickening of mucosal layer
$SM_{2\sim3}$		Low S/I mass in submucosa
MP		Discontinuity of muscle layer Thickening of muscle layer Replacement of muscle by tumor High S/I mass in muscle layer
S (A)	Irregular outer surface of bowel wall	Discontinuity of outer longitudinal muscle layer

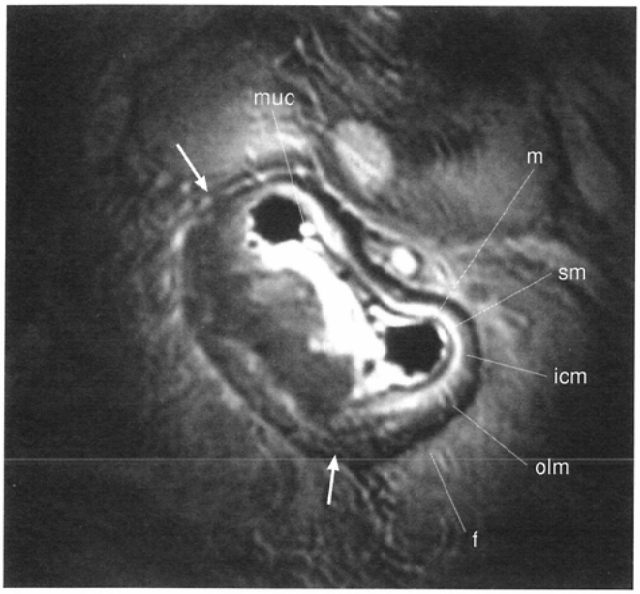

Fig. 2 MRI appearance of the normal rectal wall and its histological correlation. Six-layer architecture is resolved on a T2-weighted axial image (FSE: TR/TE 3700/104): from inside, bright mucus (muc), dark mucosal layer including mucosa and muscularis mucosa (m), bright submucosa (sm), intermediate inner circular muscle layer (icm), dark outer longitudinal muscle layer (olm), and bright perirectal fat tissue (f). The normal laminar structure is interrupted by tumor (arrows).

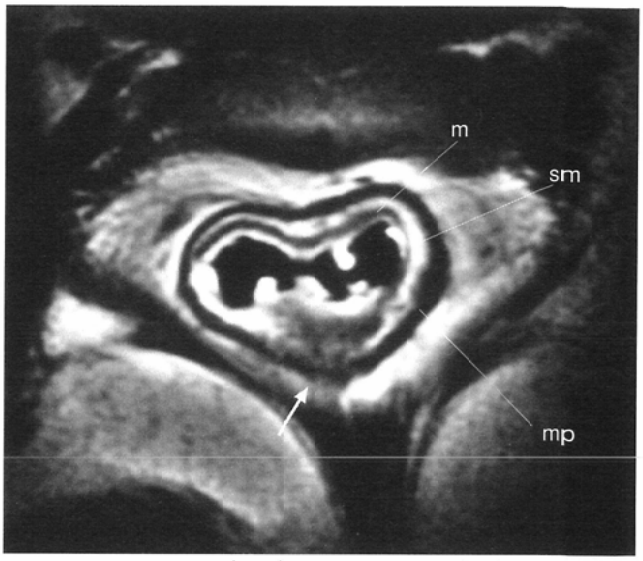

Fig. 3 In some cases (4/55), the submucosa (sm) appears very bright between the dark mucosa (m) and muscle layer (mp) on noncontrast T1-weighted images, providing natural contrast. A tumor located at the posterior wall infiltrates the submucosa and superficial muscle layer (arrow).

hypointense muscle layer, replacement of the muscle by tumor, or a high signal intensity mass in the muscle layer on the T2-weighted image; S(A)-carcinoma: irregular outer surface of the bowel wall on the T1-weighted image and discontinuity of outer most hypointense layer on the T2-weighted image.

The MRI criteria with which the diagnosis of lymph node metastasis was made were that the lymph node was larger than 5 mm in diameter and/or more spherical and irregular in shape on the MR images taken by the endorectal coil or the phased array coil.

Results

The cases consisted of eight patients with carcinomas limited to the mucosa, or m-carcinoma, 12 with carcinomas involving the submucosa, or sm-carcinoma, 21 with carcinomas spreading into the muscularis propria, or mp-carcinoma, and 14 with carcinomas penetrating through the muscularis propria, or s(a)-carcinoma, with respect to the succeeding histopathologic examination.

1. Visualization of Normal Architecture of Bowel Wall

Figure 2 demonstrates a T2-weighted image of rectal cancer obtained with the endorectal surface coil. On this image, the normal rectal wall is visualized as a six-layer structure at the left anterior side of the rectum. The inner most high signal intensity represents mucus and adjacent debris, the second low signal line, the mucosa, and the third high signal intensity zone, the submucosa. The muscularis propria appears as two lines, the inner gray and the outer dark, respectively representing the inner circular muscle layer and the outer longitudinal muscle layer. The perirectal fat tissue shows a fairly high signal intensity on the T2-weighted image with FSE.

On T1-weighted images, all layers of the normal rectal wall usually appear hypointense. However, in four of 55 cases, the submucosa showed very high signal intensity on T1-weighted images, and the diagnosis of carcinomatous invasion was possible even without administration of Gd-DTPA or T2-weighted images (Fig. 3).

2. Signal Intensity of the Tumors

The signal intensity of the colorectal tumors varied according to their morphologic components[7]. The epithelial component of the tumor appeared as a low signal intensity area on T1-weighted images and showed low to intermediate signal intensity on T2-weighted images. Associated desmoplastic change appeared as low signal intensity on both T1- and T2-weighted images. Extracellular mucin was demonstrated as low signal intensity on T1-weighted images and as characteristic high signal intensity on T2-weighted images.

3. Extent of Bowel Invasion on MRI

Table 2 shows the correlation between the MR imaging and pathologic findings on the extent of intramural tumor invasion. In 45 of 55 cases (81.8%) of rectal cancer, MRI led to the correct diagnoses on the extent of tumor infiltration. M- and sm_1-carcinoma appeared as discrete thickening of the mucosal layer, and the interface between the tumor and the submucosa was smooth on the T2-weighted images (Fig. 4). $Sm_{2\text{-}3}$-carcinoma was shown to have a fuzzy boundary between the tumor and the submucosa (Fig. 5) or was depicted as a low signal intensity mass in the submucosal layer (Fig. 6). The MRI findings of muscularis propria involvement (mp) were discontinuity of the submucosa, thickening of the muscle layer, or a high sig-

Table 2 Correlation of endorectal MR imaging and histopatholgic diagnosis of depth of carcinomatous invasion (n = 55)

MR assessment	Histopathologic diagnosis				
	m	sm1	$sm_{2\sim3}$	mp	s (a)
M, SM1	4	1	1		
$SM_{2\sim3}$	4		8	1	
MP			2	18	
S (A)				2	14
Total	8	1	11	21	14

Accuracy 81.8%. sm_1: minute submucosal invasion, $sm_{2\sim3}$: massive submucosal invasion.

nal intensity mass in the muscle layer (Fig. 7). Tumor invasion into the perirectal fat (s-carcinoma) was demonstrated as the irregular outer surface of the bowel wall on T1-weighted images and as discontinuity of the outer longitudinal muscle layer on T2-weighted images (Fig. 8). T1-weighted images with Gd-DTPA administration showed less contrast between tumor and submucosa or muscle layer than T2-weighted image sexcept for one case of mp-carcinoma.

In four cases of m-carcinoma, two of $sm_{2\sim3}$-carcinoma and two of mp-carcinoma, however, the tumor extent was overestimated. In two cases of m-carcinoma erroneously diagnosed as $SM_{2\sim3}$ based on MR images, foreign body granulomas were found in the submucosa on the microscopic sections. These were probably attributable to the endoscopic submucosal injection of tattoo by way of marking for laparoscopic surgery. In the other two cases of m-carcinoma, the submucosa was too thin to resolve in the early series when the submucosal saline injection had yet to be attempted. In two cases of $sm_{2\sim3}$-carcinoma and one of mp-carcinoma, the endorectal coil ended up being placed far from the lesion owing to hyperinflation of the inner balloon. In one case of mp-carcinoma, the tumor was located at the steep angulation, resulting in an oblique,

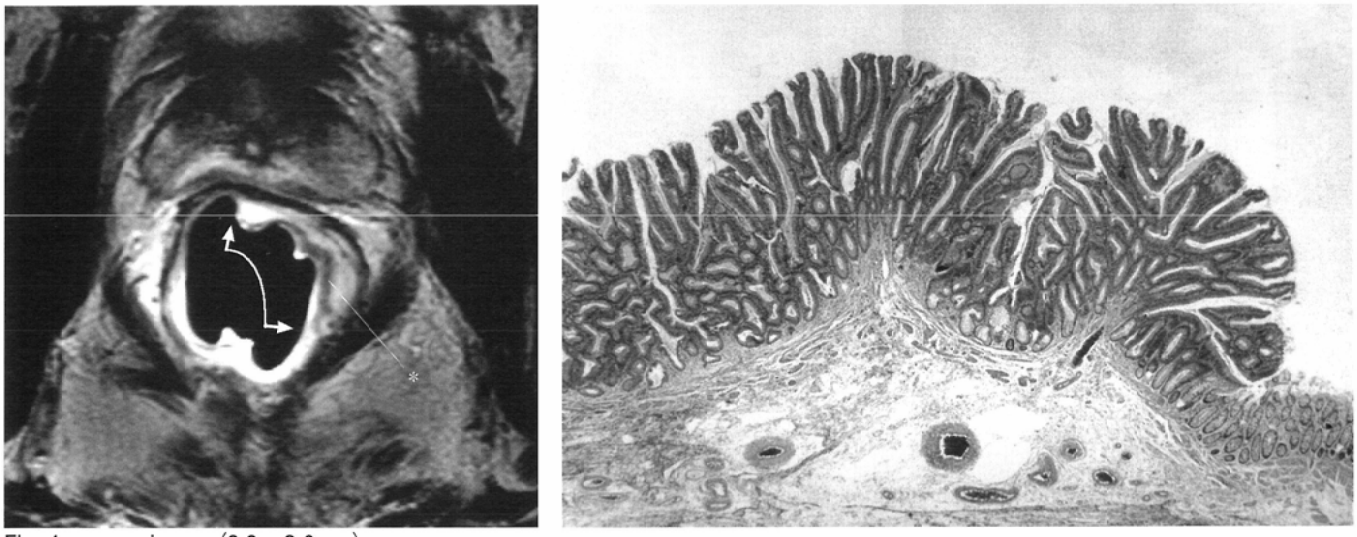

Fig. 4 m-carcinoma (3.0 × 3.0 cm).
A: Localized thickening of the mucosal layer (arrows) is clearly seen on a T2-weighted image after submucosal saline injection. Its border with the submucosa is smooth (*).
B: Well differentiated adenocarcinoma is confined to the mucosa.

A B

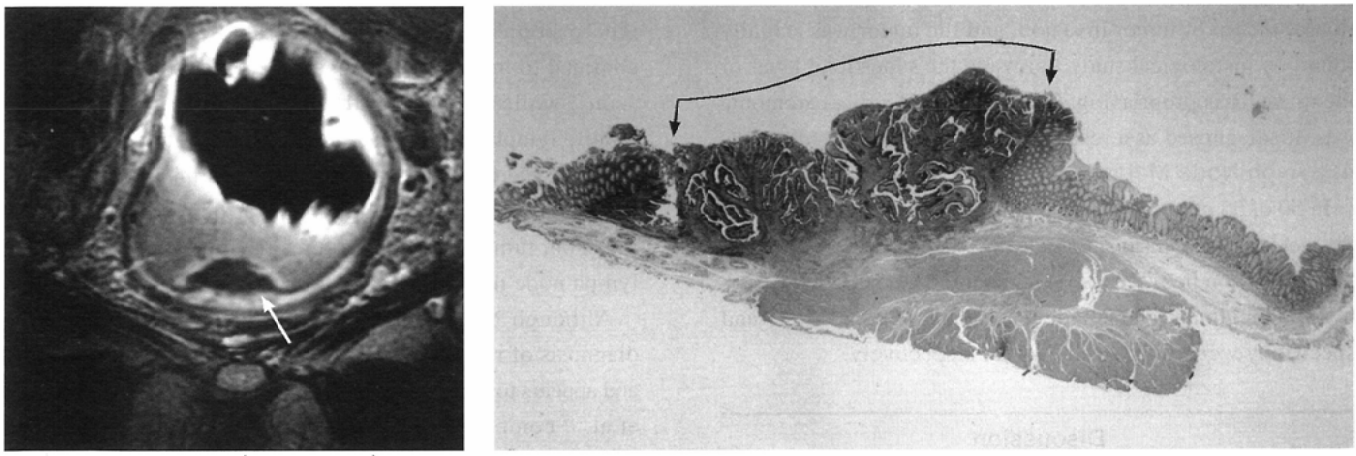

Fig. 5 sm_3-carcinoma (1.5 × 1.5 cm) after submucosal saline injection.
A: A cross-sectional T2-weighted image shows a fluffy interface at the base of the hypointense tumor (arrow) and hyperintense submucosa.
B: Carcinoma infiltrates into the submucosal layer (arrows).

A B

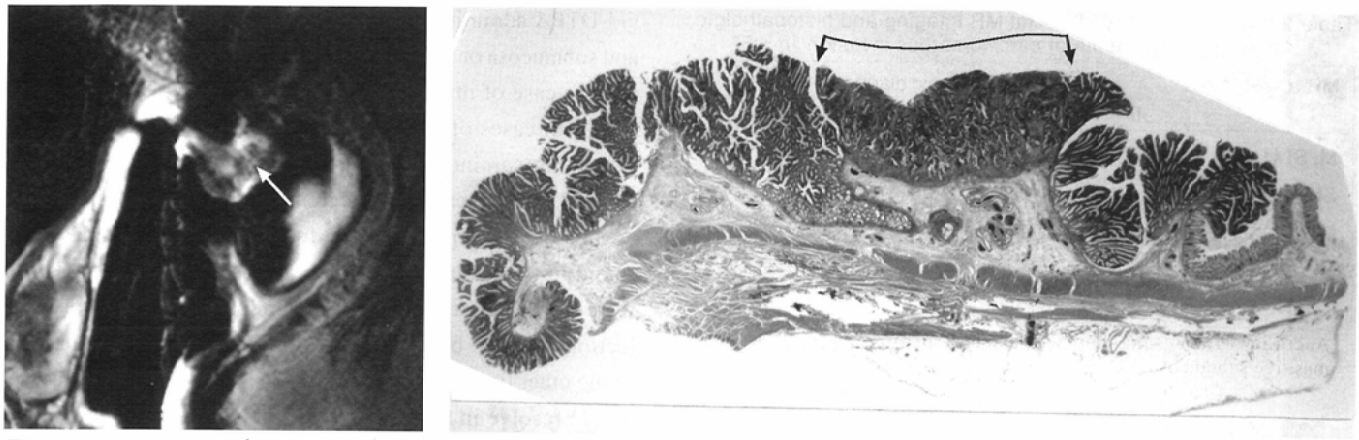

Fig. 6 sm_2-carcinoma (4.0 × 3.0 cm) after submucosal saline injection.
A: Submucosal invasion of the carcinoma is represented on a T2-weighted image as a hypointense bump (arrow) projected into the hyperintense submucosa.
B: Although most of the tumor is confined within the mucosa, it penetrates the muscularis mucosa and invades the submucosa (arrows).

A | B

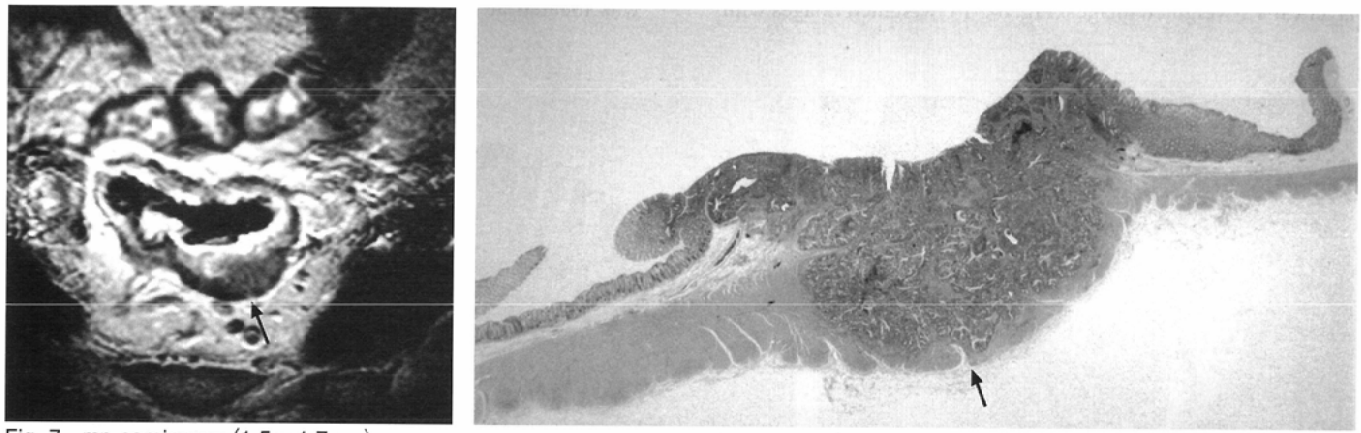

Fig. 7 mp-carcinoma (1.5 × 1.7 cm).
A: A tumor involving the dark muscle layer appears slightly brighter on a T2-weighted image. A closer look reveals that the tumor abuts the outer muscle layer at one site (arrow) as proven in (B).

A | B

rather than an optimal perpendicular, imaging plane.

In one case each of $sm_{2\sim3}$-carcinoma and mp-carcinoma, MRI diagnosis resulted in underestimation. In the case of mp-carcinoma, there was a hyperintense zone between the tumor and hypointense muscle layer on T2-weighted imaging. The hyperintense zone, however, turned out to be colloid formation at the tip of tumor invasion, and the tumor was actually found by histological study to invade the superficial layer of the muscularis propria (Fig. 9). The case of $sm_{2\sim3}$-carcinoma was misdiagnosed as a result of degraded image quality.

4. Lymph Node Metastasis

In 50 of 55 cases, lymph node dissection was performed and the materials were histopathologically examined. Table 3 shows the correlation between the MR imaging and pathologic diagnoses on regional lymph node metastasis. The sensitivity and specificity were 78.9% and 74.1%, respectively.

Discussion

The chance of tumor recurrence and the overall prognosis of rectal cancer are known to correlate positively with the extent of carcinomatous invasion within the bowel wall and the presence of regional lymph node metastasis[8)-12)]. The development of new surgical procedures for rectal cancer has made an accurate preoperative evaluation of tumor staging and lymph node metastasis a prerequisite. Endoscopic polypectomy, endoscopic mucosal resection, transanal resection or laparoscopic resection should be applied to those tumors confined to the mucosa or superficial layer of the submucosa (sm_1), while the cases of deeper tumor penetration usually require lymph node dissection with or without nerve-sparing surgery. Therefore, the most important determinants in selecting a surgical procedure are the penetration of carcinomatous invasion, tumor location (distance from the anal verge), and lymph node metastasis.

Although MR imaging results have been reported in the diagnosis of rectal cancer, their accuracy varies considerably and appears to depend heavily on technical conditions. Zerhouni et al.[13)] compared MR imaging and CT in 365 patients with colorectal carcinoma and reported that the accuracy of CT (74%) in tumor staging was better than that of MR imaging using a whole-body coil (58%). De Lange et al.[14)], using a

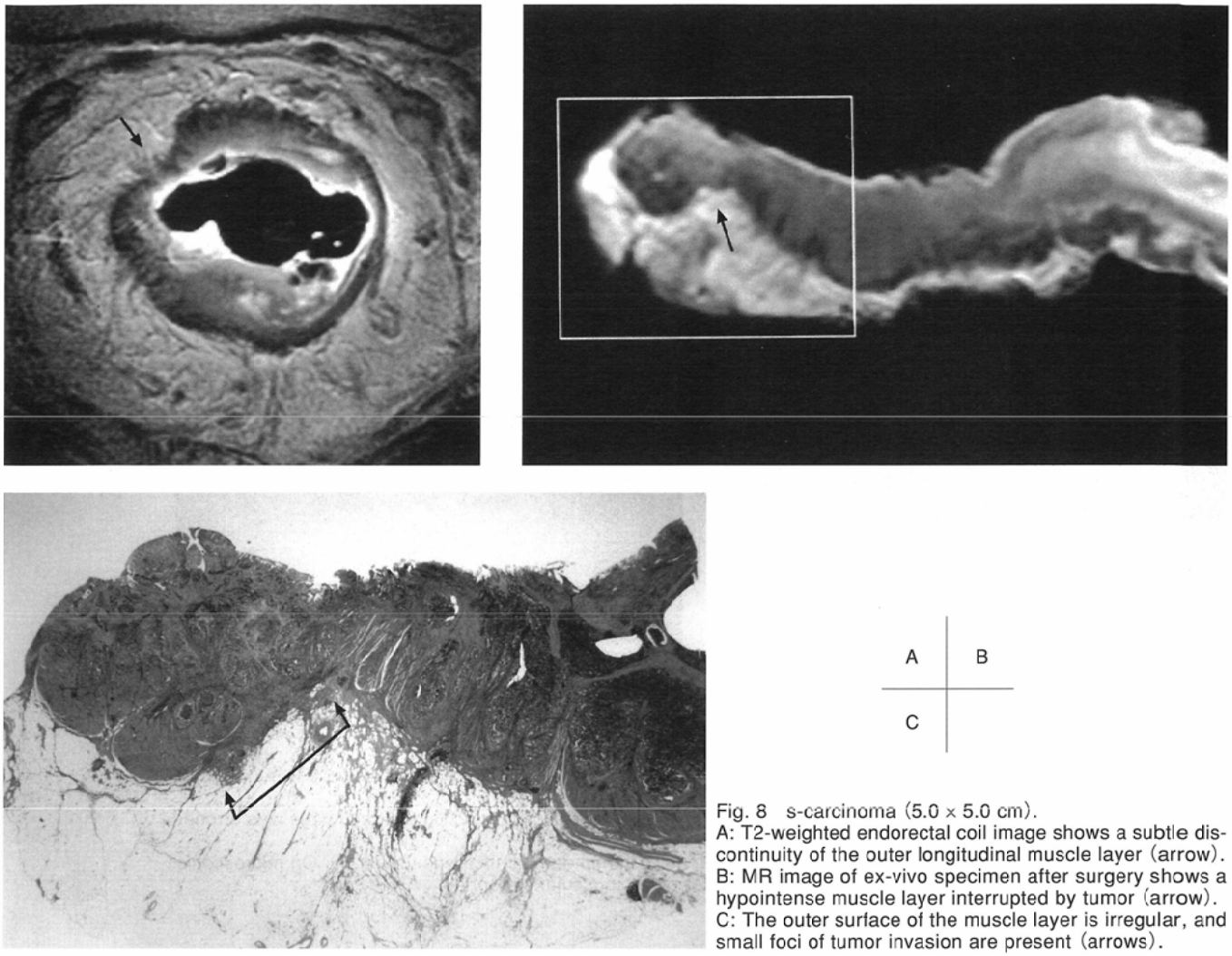

Fig. 8 s-carcinoma (5.0 × 5.0 cm).
A: T2-weighted endorectal coil image shows a subtle discontinuity of the outer longitudinal muscle layer (arrow).
B: MR image of ex-vivo specimen after surgery shows a hypointense muscle layer interrupted by tumor (arrow).
C: The outer surface of the muscle layer is irregular, and small foci of tumor invasion are present (arrows).

17-cm Helmholtz coil, reported accuracy of 89.6% in staging local extent with the modified Asler-Coller staging classification. Schnall et al.[15] reported diagnostic accuracy of 81% in T-staging using endorectal MR imaging, while Pegios et al. reported a similar rate of 85%[16].

T1-weighted images are most appropriate for defining tumor extension beyond the intestinal wall, because the outer surface of the intestinal wall is usually well-delineated as a hypointense line against the hyperintense perirectal fat. However, it should be noted that an irregular outer surface of the bowel wall is not a pathognomonic sign of extramural tumor invasion. Even in tumors contained within the bowel wall, thin radiating structures representing fibrous tissues were occasionally seen in the perirectal fat. Sometimes a tumor pushes the muscle layer without penetration. A more reliable finding suggestive of extramural tumor invasion is discontinuity of the outer longitudinal muscle layer, which is well-visualized as a very dark line on T2-weighted imaging (Fig. 8).

In four exceptional cases in our series, the submucosal layer showed high signal intensity on the T1-weighted images (Fig. 3). The cause for this was unclear from the viewpoint of histopathology as well. The submucosal layer was enhanced as an area of high signal intensity on T1-weighted images with Gd-DTPA administration. The muscle layer, however, was enhanced as well, and the difference in contrast between the two layers was small, because we used a spin echo sequence for the T1-weighted image and the scanning time was about three minutes. Therefore, the evaluation of tumor invasion was based on the T2-weighted images in this study.

The most crucial distinction in the tumor penetration of early colorectal cancer lies between minute (sm_1) and massive (sm_{2-3}) submucosal invasion. Inoue et al.[17] reviewed 357 cases of cancer infiltrating into the submucosal layer and found that 18 cases (5.0%) were positive for lymph node metastasis. The penetration of carcinomatous invasion was sm_2 or deeper in all these cases (sm_3 ina bout 90%). Sakai et al.[18] reported similar clinical data from our institution. We concluded that local resection including endoscopic polypectomy was the treatment of choice for the group with minute submucosal invasion (sm_1). The diagnostic accuracy of for m- and sm_1-carcinoma and sm_{2-3}-carcinoma was 65% (13 out of 20 cases) with MRI. This relatively low figure is attributable mainly to the fact that the submucosal layer is too thin to resolve with current MRI techniques.

To make the submucosa physically thicker, we endoscopi-

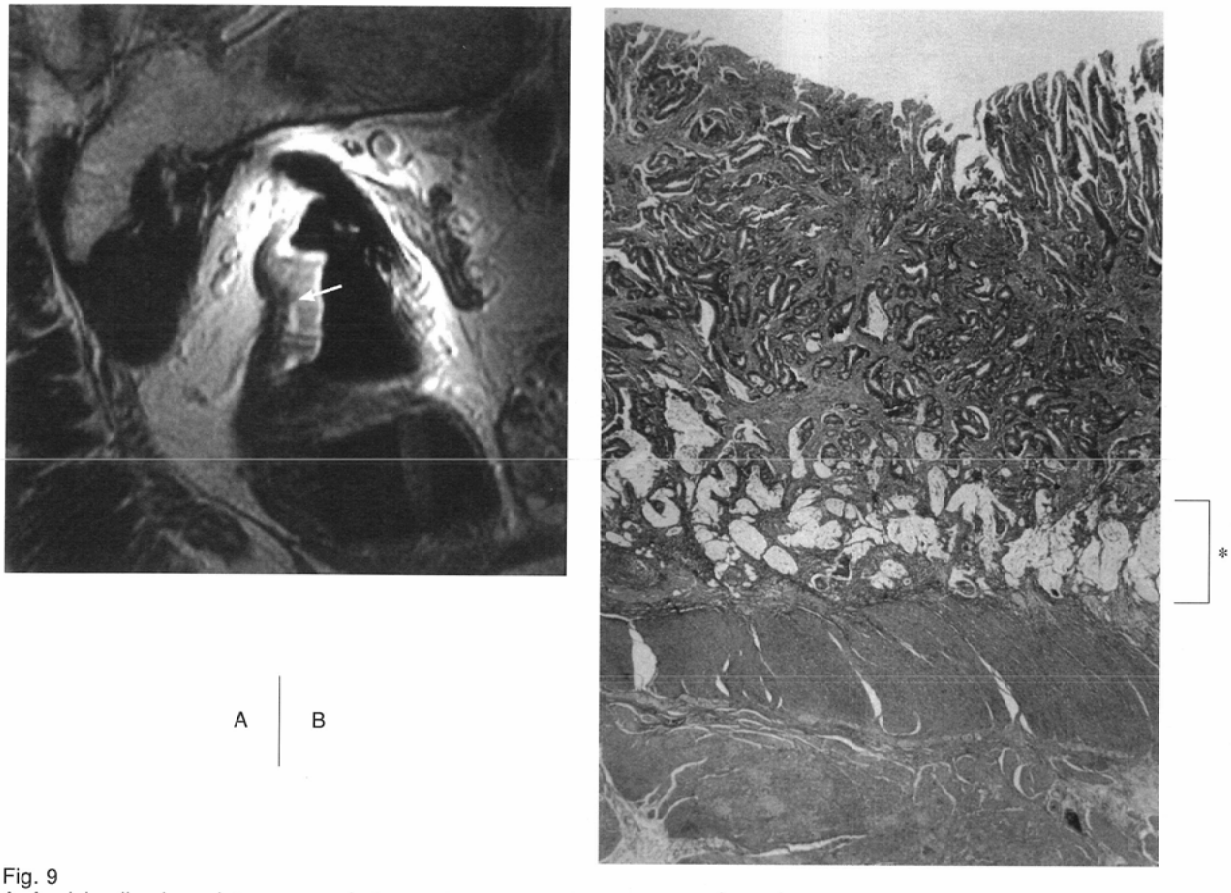

Fig. 9
A: A misleading hyperintense zone between the tumor and muscle layer (arrow) on a T2-weighted image was erroneously interpreted as cancer-free submucosa.
B: This hyperintense zone turned out to be a colloid formation at the tip of the cancerous tissue (*). On microscopic section, the tumor was seen to infiltrate the superficial layer of the muscularis propria.

cally injected saline into the submucosa before inserting the endorectal coil. Figure 10 illustrates the method of submucosal saline injection, and Figure 11 shows the differences among m- and sm_1-carcinoma, $sm_{2\sim3}$-carcinoma, and mp-carcinoma. Figure 12 compares pre-(A) and post-submucosal injection (B) T2-weighted images. With the saline injection, the evaluation of tumor penetration was easier and more accurate. The signs indicative of submucosal tumor invasion, best observed on T2-weighted images, were a fluffy boundary between the mucosa (tumor) and submucosa (Fig. 5) or direct visualization of the invasion, which was often seen as a bump projecting into the hyperintense submucosa (Fig. 6).

The accuracy of staging rectal cancer with endoscopic ultrasound (EUS) or transrectal ultrasound (TRUS) varies from 60% to 88%[19)-27)]. Hulsmans et al. pointed out the difficulty in differentiating between tumors limited to the muscularis propria (T2) and those penetrating further into the perirectal fat (T3). Fifty percent of pT2 tumors were overstaged as pT3 due to inflammatory (desmoplastic) reaction or retraction of the muscularis propria[26)]. In contrast, the signal intensity of the outer longitudinal muscle layer is darker than that of tumor on T2-weighted MR images. MR imaging can detect a very small tumor penetrating the perirectal fat from the discontinuity in the very dark outer longitudinal muscle layer on T2-weighted images. Other advantages of MR imaging over EUS include a larger field of view and arbitrarily selectable slice planes that make it easier to determine not only the stage of the tumor but also its location, and to produce the slice plane exactly perpendicular to the rectal wall, for the best view.

Table 3 Correlation of in-vivo MR imaging and histopathologic diagnosis of regional lymph node metastasis in rectal carcinoma (n = 50)

MR assessment	Histopathologic diagnosis	
	n0	n1
N0	23	4
N1	8	15

Sensitivity 78.9%, Specificity 74.1%.

The endorectal coils used in this study were similar to the prostate probe developed by Schnall et al.[28)], but were made in our laboratory with some modifications to accommodate rectal lesions. Oval-shaped surface coils, 6×3 cm to 12×6 cm in size, were mounted between the outer and inner balloons. The inner balloon was used to extend the coil to a designed, tuned shape. These balloons were softer and more ellipsoidal in cross-section than those for prostate coils, so as to keep the coils closer to the lesion. The coil shaft is covered with a thick silicone tube and is not rigid. Although the endorectal coil

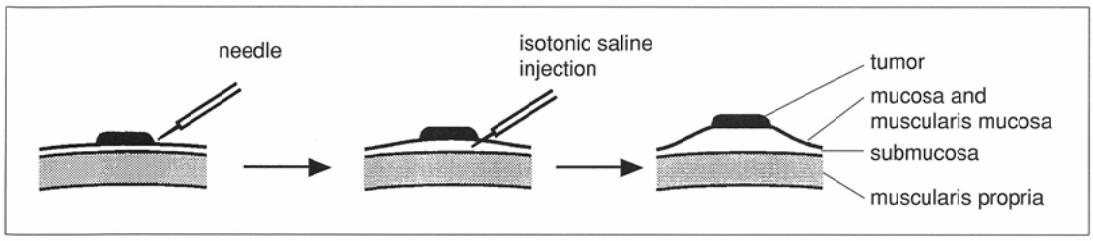

Fig. 10 Submucosal saline injection. A small amount of saline is injected into the submucosa by a needle delivered through the forceps channel of the endoscope, for better mucosa-muscularis propria separation.

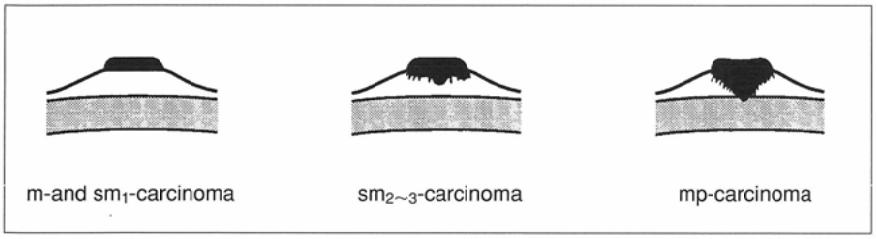

Fig. 11 Schematic distinction among m- and sm1-carcinoma, $sm_{2\sim3}$-carcinoma, and mp-carcinoma after submucosal saline injection. Note the fluffy boundaries between the tumor-mucosa and submucosa in $sm_{2\sim3}$-carcinoma.

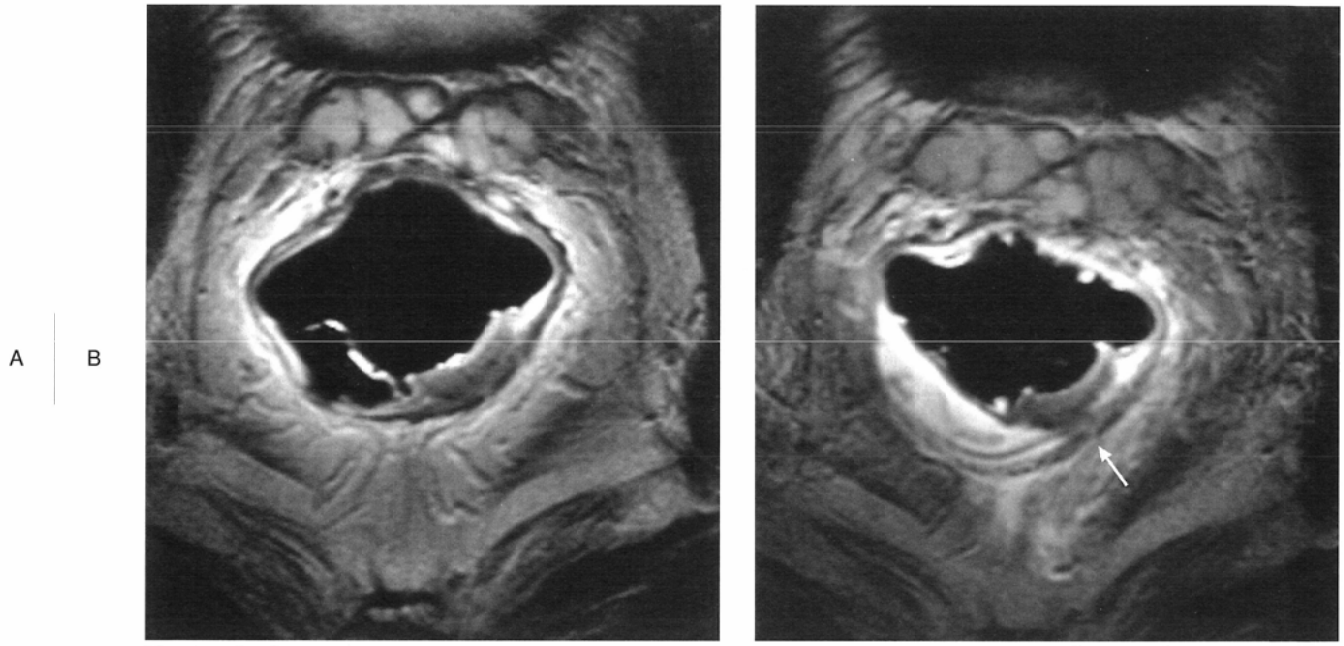

Fig. 12 A minute cancerous invasion is better appreciated after submucosal saline injection (B: arrow) than before the procedure (A) (T2-weighted images).

improved the signal-to-noise ratio, we found that image quality was not quite satisfactory with overly distended bowels owing to excessive coil mobility, coil-object separation, and thinned bowel wall. These problems could be solved simply by air-aspiration through the drainage tube. The drainage tube was placed posterior to the coil, because the coil usually stayed close to the anterior wall of the rectum.

In some cases we had difficulty inserting the coil owing to the narrow, angulated rectum. Air-inflation into the rectum worked well in 20 cases. In seven cases, we placed the coil on the tumor located at the recto-sigmoid junction by dint of the endoscope and grasping forceps. Once the coil was properly placed, the aspiration of air was carried out through the endoscopic channel. This maneuver can transport the endo luminal coil beyond the rectum, although it requires an endoscopic technique and is somewhat complicated.

In conclusion, MR images obtained with an endorectal coil can depict intramural tumor infiltration with all the layers of the normal intestinal wall. The smoothness of the outer surface of the muscle layer on T1-weighted images and the continuity of the outer longitudinal muscle layer on T2-weighted images were most valuable in differentiating intramural carcinoma from that penetrating through the muscularis propria. Submucosal saline injection was useful in differentiating between m- and sm_1-carcinoma and $sm_{2\sim3}$-carcinoma, and between sm-carcinoma and mp-carcinoma on T2-weighted images. Endorectal MRI is advantageous in that the form of small lymph nodes above and below 5 mm in diameter can be evaluated more precisely in terms of the diagnosis of lymph node metastasis. Even if small in size, a lymph node that is more spherical or irregular in shape should be considered for the possibility of metastasis.

Our results suggest that endorectal MR imaging can improve the accuracy of staging of rectal cancer and the depiction of

tumor growth pattern. Further study will be required to evaluate the potential of endorectal coil MR imaging for the management of patients with rectal cancer, especially in comparison with endoscopic ultrasonography.

Acknowledgments

The author thanks Kyoichi Hiramatsu, M.D., Chairman of the Department of Radiology, Keio University School of Medicine, for helpful advice regarding manuscript preparation. The author also thanks Masaki Kitajima, M.D., Chairman of the Department of Surgery, and Tatsuo Teramoto, M.D., for their clinical support in patient management, and MakioMukai, M.D., Department of Clinical Pathology, for many stimulating discussions regarding MRI-histopathological correlations. Finally, the author thanks Nobuya Higuchi, M.D., for the development of the fast spin echo (multi-shot RARE) sequence in 1990 and for help in manuscript preparation.

References

1) Parks AG: Transanal technique in low rectal anastomosis. Proc R Soc Med 65: 696-700, 1972
2) Mason YA: Transsphincteric exposure for low rectal anastomosis. Proc R Soc Med 65: 974-978, 1972
3) Hager TH, Gall FP, Hermanek P: Local excision of cancer of the rectum. Dis Colon Rectum 26: 149-151, 1983
4) Phillips EH, Franklin M, Carroll BJ, et al: Laparoscopic colectomy. Ann Surg 216: 703-707, 1992
5) Moriya Y, Sugihara K. Akasu T, et al: Nerve-sparing surgery with lateral node dissection for advanced lower rectal cancer. Eur J Cancer 31A: 1229-1232, 1995
6) Colon and Rectum. (In) Sobin LH, Wittekind Ch ed: UICC: TNM classification of malignant tumors. 5th ed. 66-69, 1997, Wiley-Liss, New York
7) Imai Y, Kressel HY, Saul SH, et al: Colorectal tumors: An in vitro study of high-resolution MR imaging. Radiology 177: 695-701, 1990
8) Gunderson LL, Sosin H: Areas of failure found at operation (second or symptomatic look) following "curative surgery" for adenocarcinoma of the rectum. Cancer 34: 1278-1292, 1974
9) Moosa AR, Ree PC, Marks JE, et al: Factors influencing local recurrence after abdominoperineal resection for cancer of the rectum and rectosigmoid. Br J Surg 62: 727-730, 1975
10) Cass AW, Million RR, Pfaff WW: Patterns of recurrence following surgery alone for adenocarcinoma of the colon and rectum. Cancer 37: 2861-2865, 1976
11) Rich T, Gunderson LL, Lew R, et al: Patterns of recurrence of rectal cancer after potentially curative surgery. Cancer 52: 1317-1329, 1983
12) Moriya Y, Sugihara K, Akasu T, et al: Patterns of recurrece after nerve-sparing surgery for rectal adenocarcinoma with special reference to loco-regional recurrence. Dis Colon Rectum 38: 1162-1168, 1995
13) Zerhouni EA, Rutter C, Hamilton SR, et al: CT and MR imaging in the staging of colorectal carcinoma: Report of the Radiology Diagnostic Oncology Group II. Radiology 200: 443-451, 1996
14) De Lange EE, Fechner RE, Edge SB, et al: Preoperative staging of rectal carcinoma with MR imaging: Surgical and histopathologic correlation. Radiology 176: 623-628, 1990
15) Schnall MD, Furth EE, Rosato EF, et al: Rectal tumor stage: Correlation of endorectal MR imaging and pathologic findings. Radiology 190: 709-714, 1994
16) Pegios W, Vogl Th J, Mack MG, et al: MRI diagnosis and staging of rectal carcinoma. Abdom Imaging 21: 211-218, 1996
17) Inoue Y, Suzuki M, Yoshida K, et al: A study of submucosal carcinoma of the colon and rectum with lymph node metastases. J Jpn Soc Coloproctol 51: 159-167, 1998
18) Sakai N, Watanabe M, Teramoto T, et al: Clinicopathological analysis and therapeutic plan of early invasive colorectal cancer. Jpn J Gastroenterol Surg 30: 60-65, 1997
19) Hildebrandt U, Feifel G: Preoperative staging of rectal cancer by intrarectal ultrasound. Dis Colon Rectum 28: 42-46, 1985
20) Beynon J, Foy DMA, Roe AM, et al: Endoluminal ultrasound in the assessment of local invasion in rectal cancer. Br J Surg 73: 474-477, 1986
21) Roubein LD, David C, DuBrow R, et al: Endoscopic ultrasonography in staging rectal cancer. Am J Gastroenterol 85: 1391-1394, 1990
22) Waizer A, Powsner E, Russo I, et al: Prospective comparative study of magnetic resonance imaging versus transrectal ultrasound for preoperative staging and follow-up of rectal cancer. Dis Colon Rectum 34: 1068-1072, 1991
23) Glaser F, Schlag P, Herfarth Ch: Endorectal ultrasonography for the assessment of invasion of rectal tumors and lymph node involvement. Br J Surg 77: 883-887, 1990
24) Sentovich SM, Blatchford GJ, Falk PM, et al: Transrectal ultrasound of rectal tumors. Am J Surg 166:638-642, 1993
25) Thaler W, Watzka S, Martin F, et al: Preoperative staging of rectal cancer by endoluminal ultrasound vs. magnetic resonance imaging. Dis Colon Rectum 37: 1189-1193, 1994
26) Hulsmans FJH, Tio TL, Fockens P, et al: Assessment of tumor infiltration depth in rectal cancer with transrectal sonography: Caution is necessary. Radiology 190: 715-720 , 1994
27) Meyenberger C, Huch Boni RA, Bertschinger P, et al: Endoscopic ultrasound and endorectal magnetic resonance imaging: A prospective, comparative study for preoperative staging and follow-up of rectal cancer. Endoscopy 27: 469-479, 1995
28) Schnall MD, Lenkinski RL, Pollack HM, et al: Prostate: MR imaging with an endorectal surface coil. Radiology 172: 570-574, 1989